Silencing of MAP4K4 by short hairpin RNA suppresses proliferation, induces G1 cell cycle arrest and induces apoptosis in gastric cancer cells

YUAN-FEI LIU, GUO-QIANG QU, YUN-MIN LU, WU-MING KONG, YUAN LIU, WEI-XIONG CHEN and XIAO-HONG LIAO

Department of Gastroenterology, Shanghai Jiao Tong University Affiliated Sixth People's Hospital, Shanghai 200233, P.R. China

Received November 6, 2014; Accepted August 17, 2015

DOI: 10.3892/mmr.2015.4510

Abstract. Gastric cancer (GC) is the second most common cause of cancer-associated mortality worldwide. Previous studies suggest that mitogen-activated protein kinase kinase kinase kinase isoform 4 (MAP4K4) is involved in cancer cell growth, apoptosis and migration. In the present study, bioinformatics analysis and reverse transcription-quantitative polymerase chain reaction were performed to determine if MAP4K4 was overexpressed in GC. The knockdown of MAP4K4 by RNA interference in GC cells markedly inhibited cell proliferation, which may be mediated by cell cycle arrest in the G1 phase. The silencing of MAP4K4 also induced cell apoptosis by increasing the ratio of Bax/Bcl-2. In addition, Notch signaling was markedly reduced by MAP4K4 silencing. The results of the present study suggested that inhibition of MAP4K4 may be a therapeutic strategy for GC.

Introduction

Gastric cancer (GC) is one of the most common forms of cancer and is the second highest cause of cancer-associated mortality worldwide (1). Due to its aggressive growth and the lack of effective treatment options, the disease has a high mortality rate, with a 5-year survival rate of ~20% (2). It is of great importance to identify novel biomarkers for an early diagnosis, targeted treatment and prognosis evaluation in GC.

Mitogen-activated protein kinases (MAPKs) are a family of conserved serine/threonine protein kinases, which are essential in transmitting extracellular signals into the cytoplasm (3). MAPKs are important in modulating and regulating several crucial cellular processes, including growth, migration, differentiation, apoptosis and stress-associated responses. MAPK kinase kinase kinase isoform 4 (MAP4K4; also termed hepatocyte progenitor kinase-like/germinal center kinase-like kinase) is involved in the regulation of cell motility, rearrangement of the cytoskeleton and cell proliferation (4-7). Previous studies revealed that MAP4K4 is overexpressed in numerous types of human cancer (5,8-10). In addition, the overexpression of MAP4K4 is a prognostic marker for stage II pancreatic ductal (8) and lung (10) adenocarcinomas. In particular, silencing of MAP4K4 by small interfering RNA inhibits the invasion and migration of cancer cells from different anatomic origins, including breast cancer, prostate cancer, ovarian cancer and malignant melanoma (4). The suppression of MAP4K4 protein expression in hepatocellular carcinoma cells reduces cell proliferation, inhibits the cell cycle progression and increases cell apoptosis (9). These results suggest an involvement of MAP4K4 in cancer progression. However, little is known about the expression pattern and biological functions of MAP4K4 in GC.

To investigate the roles of MAP4K4 in GC, the protein was overexpressed in GC and normal tissue. The effects of knocking down MAP4K4 on the proliferation, invasion and apoptosis of GC cells were assessed, and a putative mechanism was also investigated. The present study provided for the first time, to the best of our knowledge, an assessment of the overexpression of MAP4K4 in GC, and how this may be an effective therapeutic target for this disease.

Materials and methods

Bioinformatics analysis. The Cancer Genome Atlas (TCGA) RNA sequencing (RNA-Seq) information and corresponding clinical data, were downloaded from the TCGA website (http://cancergenome.nih.gov), following approval of this project by the consortium of Shanghai Jiao Tong University Affiliated Sixth People's Hospital (Shanghai, China). RNA-Seq analysis used data from 249 stomach cancer samples and 33 adjacent normal tissues. To gain further insights into the biological pathways involved in the pathogenesis of stomach cancer via the MAP4K4 pathway, a gene set enrichment

Correspondence to: Dr Guo-Qiang Qu, Department of Gastroenterology, Shanghai Jiao Tong University Affiliated Sixth People's Hospital, 600 Yishan Road, Shanghai 200233, P.R. China
E-mail: quguoqiangwz@126.com

Key words: gastric cancer, MAP4K4, G1 arrest, apoptosis, Notch signaling

analysis (GSEA) was performed. The gene sets demonstrating a false discovery rate of 0.25, a well-established cut-off for the identification of biologically relevant genes, were considered enriched between the classes under comparison.

Cancer specimens. Specimens of GC and paired non-cancerous tissues were obtained from 25 patients, including 8 females and 17 males, aged between 42 and 83 years (median age, 64 years). All tissues were snap-frozen in liquid nitrogen immediately following resection. Written informed consent was obtained from the patients.

RNA extraction and reverse transcription-quantitative polymerase chain reaction (RT-qPCR). The total RNA was extracted using TRIzol® reagent (Invitrogen Life Technologies, Carlsbad, CA, USA), according to the manufacturer's instructions. The complementary DNA was synthesized using a cDNA synthesis kit (Thermo Fisher Scientific Inc., Rockford, IL, USA). RT-qPCR analyses were performed using SYBR Green (Takara Biotechnology Co., Ltd., Dalian, China), and data collection was conducted using an ABI 7500 (Applied Biosystems Life Technologies, Foster City, CA, USA). RT-qPCR was performed to detect the mRNA expression levels of the genes, as indicated below. GAPDH was used an internal control for normalization. The gene expression was calculated using the $2^{-\Delta\Delta Ct}$ method (11). The primers (Sangon Biotech Co., Ltd., Shanghai, China) used were as follows: MAP4K4, forward: 5'-GATGAGGAGGACGACGATGTG-3' and reverse: 5'-GTCTGGCGGACGATTAGAGTG-3'; GAPDH, forward: 5'-CACCCACTCCTCCACCTTTG-3' and reverse: 5'-CCACCACCCTGTTGCTGTAG-3'; Notch2, forward: 5'-TGAGTGTCTGAAGGGTTATG-3' and reverse: 5'-TGAAGCCTCCAATCTTATCC-3'; Notch3, forward: 5'-CATCCGAAACCGCTCTAC-3' and reverse: 5'-GTCTCCTCCTTGCTATCC-3'; Hes1, forward: 5'-CAGTTTGCTTTCCTCATTC-3' and reverse: 5'-TCTCCCAGTATTCAAGTTC-3'. The PCR cycling conditions were as follows: 95˚C for 10 min, followed by 40 cycles at 95˚C for 15 sec and 60˚C for 45 sec and a final extension step of 95˚C for 15 sec, 60˚C for 1 min, 95˚C for 15 sec and 60˚C for 15 sec.

Cell lines. All culture media were supplemented with 10% fetal bovine serum (FBS; Invitrogen Life Technologies), 100 mg/ml penicillin G (Invitrogen Life Technologies) and 50 μg/ml streptomycin (Invitrogen Life Technologies). The BGC-823, SGC-7901 and AGS GC cell lines, and MKN-28 cells (all obtained from the Institute of Biochemistry and Cell Biology, Shanghai, China) were cultured in RPMI-1640 medium (Invitrogen Life Technologies). The MGC-803 and HEK-293T cells were cultured in Dulbecco's modified Eagle's medium (DMEM; Invitrogen Life Technologies). All cells were maintained at 37˚C in 5% CO_2.

RNA interference (RNAi) and construction of stable cell lines. A total of three short hairpin (sh)RNAs (Sangon Biotech Co., Ltd.) targeting nucleotide positions 5923-5945 (AAGATGGAAATGGATGTTTCA; termed MAP4K4-Ri-1), 602-624 (AATACTCTCATCACAGAAACA; termed MAP4K4-Ri-2) and 3779-3801 (AACGCAATGACAAGGTGTTCT; termed MAP4K4-Ri-3) of human MAP4K4 mRNA were cloned into a lentiviral vector (PLKO.1-EGFP; Sangon Biotech Co., Ltd.). A non-specific scramble shRNA sequence was used as the negative control (Sangon Biotech Co., Ltd.). The constructs were subsequently transfected into HEK-293T cells with lentiviral packaging vectors using Lipofectamine 2000 (Invitrogen Life Technologies), according to the manufacturer's instructions. The viruses were collected at 48 h following transfection, and were used to infect the BGC-823 cells. All assays were performed 48 h following infection.

Western blotting. The total cell lysates were extracted using radioimmunoprecipitation buffer, containing 50 mmol/l Tris-HCl (pH 8.8),150 mmol/l NaCl, 1% Triton X-100, 0.1% SDS, 1% deoxycholic acid sodium). The protein concentration was measured using a bicinchoninic acid protein assay kit (Pierce Biotechnology, Inc., Rockford, IL, USA), and absorbance was measured using a microplate reader (SM600 Labsystem; Shanghai Utrao Medical Instrument Co., Ltd., Shanghai, China). Equal quantities of cell lysates were subjected to electrophoresis using 10 or 15% sodium dodecyl sulfate-polyacrylamide gel electrophoresis and transferred to polyvinylidene fluoride membranes (Sigma-Aldrich, St. Louis, MO, USA), followed by blocking in fat-free milk overnight at 4˚C. The membranes were subsequently incubated with primary antibodies overnight at 4˚C, followed by incubation with horseradish peroxidase-conjugated goat anti-rabbit/anti-mouse secondary antibodies (cat nos. A0208 and A0216; dilution 1:1,000; Beyotime Institute of Biotechnology, Haimen, China) for 1 h at 37˚C, prior to being washed three times with Tris-buffered saline containing 20% Tween (Amresco, Solon, OH, USA). Rabbit polyclonal antibodies against Notch2 (cat. no. ab137665; 1:600), Notch3 (cat. no. ab178948; 1:20,000) and MAP4K4 (cat. no. ab155583; 1:1,000) were purchased from Abcam (Cambridge, MA, USA). Rabbit monoclonal antibodies against GAPDH (cat. no. 5174; 1:1,500) and Hes1 (cat. no. 11988; 1:1,000) were purchased from Cell Signaling Technology, Inc. (Danvers, MA, USA). Rabbit polyclonal antibodies against Bcl-2 (cat. no. sc-492; 1:150) and Bax (cat. no. sc-493; 1:100) were purchased from Santa Cruz Biotechnology, Inc. (Santa Cruz, CA, USA). The blots were visualized using enhanced chemiluminescence (Millipore, Billerica, MA, USA) and signals were quantified by densitometry (Quantity One software version 4.62; Bio-Rad Laboratories, Inc., Hercules, CA, USA).

Cell proliferation assay. The Cell Counting kit-8 (CCK-8; Dojindo Laboratories, Kumamoto, Japan) was used to detect cell proliferation. Briefly, BGC-823 cells were seeded into 96-well plates at a density of $3x10^3$ cells/well. The BGC-823 cells were subsequently infected with MAP4K4-RNAi virus or negative control virus (Neg.) following culture overnight. At the indicated time points, CCK-8 solution (10 μl in 100 μl DMEM) was added to each well and incubated for 1 h at 37˚C. Optical density (OD) values at 450 nm were measured using a microplate reader (SM600 Labsystem; Shanghai Utrao Medical Instrument Co., Ltd.

Cell cycle analysis. The cell cycle was assessed by flow cytometric analysis using propidium iodide (PI; Sigma-Aldrich)

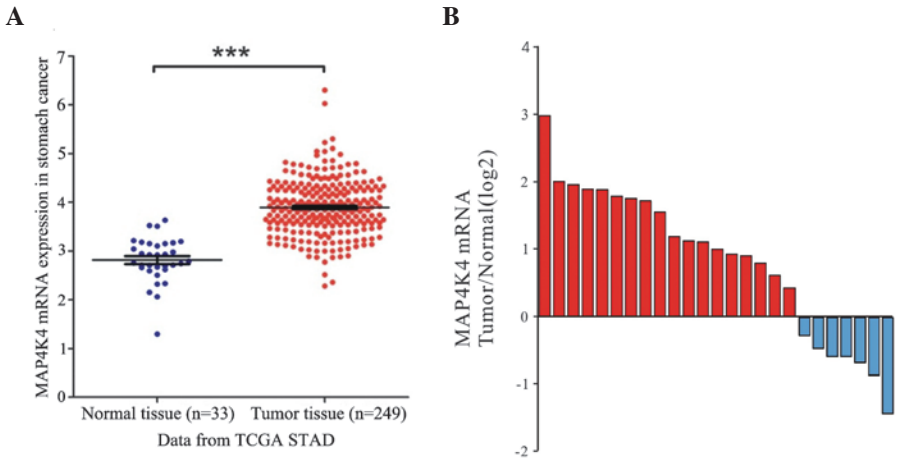

Figure 1. MAP4K4 is overexpressed in GC. (A) RNA-Seq analysis of the mRNA expression levels of MAP4K4 in the stomach tumor and normal tissues. The RNA-Seq analysis data was downloaded from the TCGA website. P<0.0001 indicated that MAP4K4 mRNA was more significantly expressed in stomach cancer tissues compared with the normal tissues. (B) The mRNA level of MAP4K4 in 25 pairs of gastric tumor and normal tissue was detected by reverse transcription-quantitative polymerase chain reaction. A positive value for $\log_2$ (tumor/normal) on the y-axis indicates an increased level of expression, whereas a negative $\log_2$ indicates a decreased level of expression of MAP4K4 mRNA in the tumor tissue. The MAP4K4 mRNA was significantly overexpressed in gastric tumor tissues as compared with the normal tissues (***P<0.001). MAP4K, mitogen-activated protein kinase kinase kinase kinase 4; TCGA, The Cancer Genome Atlas; STAD, stomach adenocarcinoma.

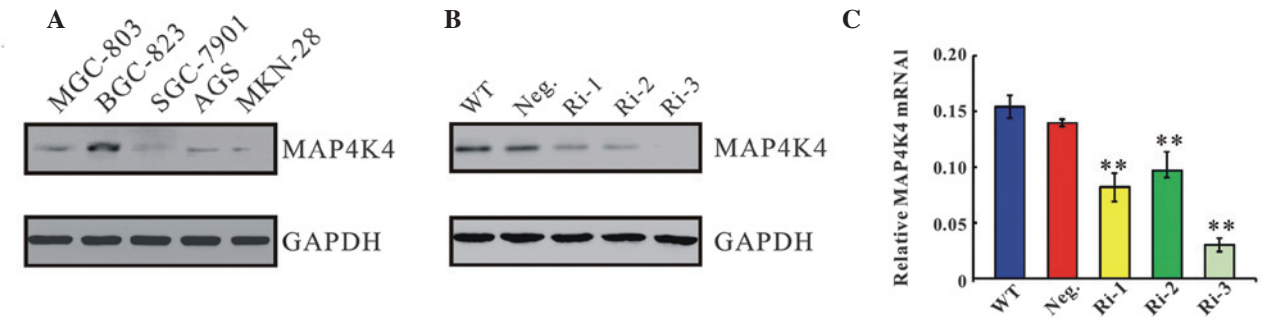

Figure 2. MAP4K4 expression is suppressed by RNAi in BGC-823 cells. (A) The protein expression of MAP4K4 in five GC cell lines (MGC-803, BGC-823, SGC-7901, AGC and MKN-28) was detected by western blotting. GAPDH was used as loading control. The BGC-823 cells demonstrated the highest expression of MAP4K4, and were subsequently selected for further analysis. (B) Western blotting and (C) reverse transcription-quantitative polymerase chain reaction demonstrated the efficiency of MAP4K4 knockdown. **P<0.01, vs. WT group. WT, wild-type; Neg., negative control; Ri-1, Ri-2 and Ri-3, MAP4K4-shRNA-1, -2 and -3; MAP4K4, mitogen-activated protein kinase kinase kinase kinase 4.

staining on a flow cytometer (BD Accuri C6, software version 1.0.264.21; BD Biosciences, Franklin Lakes, NJ, USA). Briefly, the BGC-823 cells were seeded into 6-well plates, infected with the indicated virus and cultured for 48 h. The cells were collected and fixed in 70% ethanol at -20˚C overnight. The cells were subsequently washed in phosphate-buffered saline (PBS) and resuspended in staining solution, containing 20 μg/ml PI and 200 μg/ml RNase A. All experiments were performed in triplicate and 30,000 cells were analyzed per sample.

Annexin V/PI staining and flow cytometric analysis. Annexin V/PI staining (BD Biosciences) and flow cytometric analysis were performed, according to the manufacturer's instructions. Briefly, the BGC-823 cells were seeded into 6-well plates, infected with the indicated virus and cultured for 48 h. The cells were subsequently collected by trypsinization (JRDUN Biotechnology, Shanghai, China) and incubated with annexin V-fluorescein isothiocyanate (FITC) and PI, prior to analysis by a flow cytometry. The early apoptotic cells, which were stained with FITC and emit green fluorescence, are represented in the lower right quadrant of the fluorescence-activated cell sorting histogram, and the late apoptotic cells, which were stained with FITC and PI, emit red-green fluorescence and are represented in the upper right quadrant of the histogram.

In vitro invasion assay. The upper well of the Transwell (Corning, Inc., Corning, NY, USA) was coated with Matrigel (BD Biosciences) at 37˚C in a 5% CO_2 incubator for 1 h. The cells were serum-starved for 24 h and subsequently, $5x10^4$ cells in 500 μl serum-free DMEM were seeded into the upper well of the transwell chamber. Cell culture medium, supplemented with 10% FBS (750 μl), was added into the lower well of the chamber. Following 48 h incubation, the cells in the upper well were removed with a cotton swab. The cells, which migrated into the lower well, were washed with PBS, fixed in 3.7% paraformaldehyde and stained with 0.2% crystal violet (JRDUN Biotech). Images of the cells were captured and cell numbers were counted

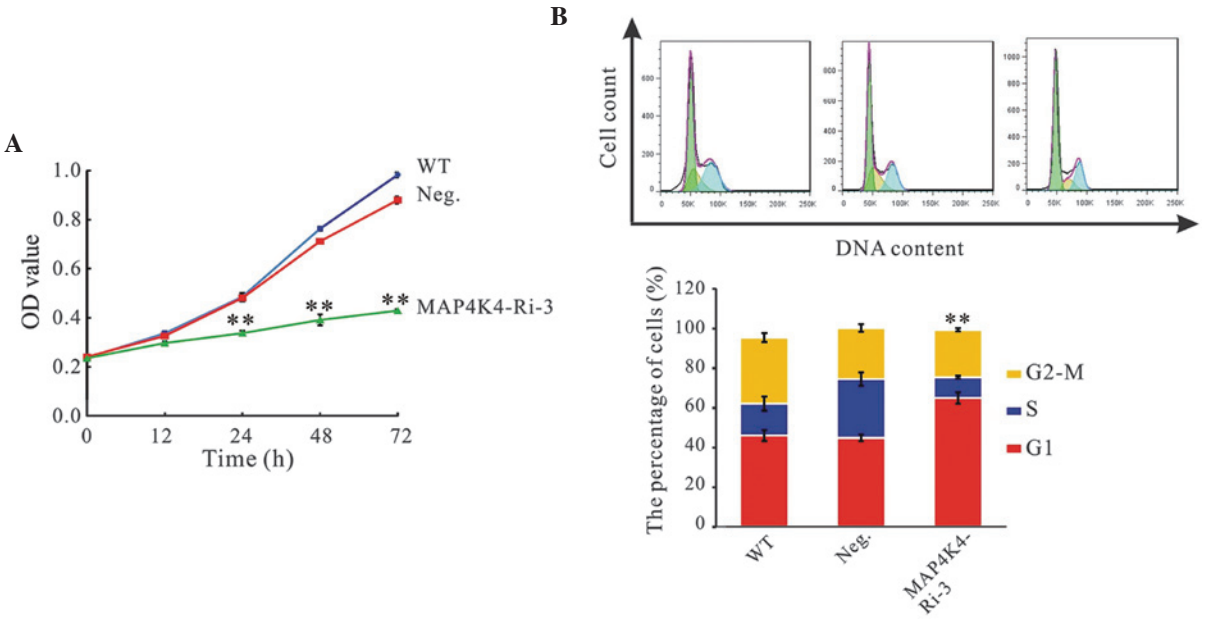

Figure 3. MAP4K4 knockdown impairs cell proliferation and the cell cycle. (A) The results of the CCK-8 assay performed in the control cells and MAP4K4 knockdown cells are shown. (B) The graph depicts the percentages of cells in the G1, S and G2-M phases for each sample at 48 h following viral infection. The data are expressed as the mean ± standard deviation (**P<0.01). WT, wild type; Neg., negative control; MAP4K4-Ri-3, MAP4K4-shRNA-3 virus-infected cells; OD, optical density; sh, short hairpin.

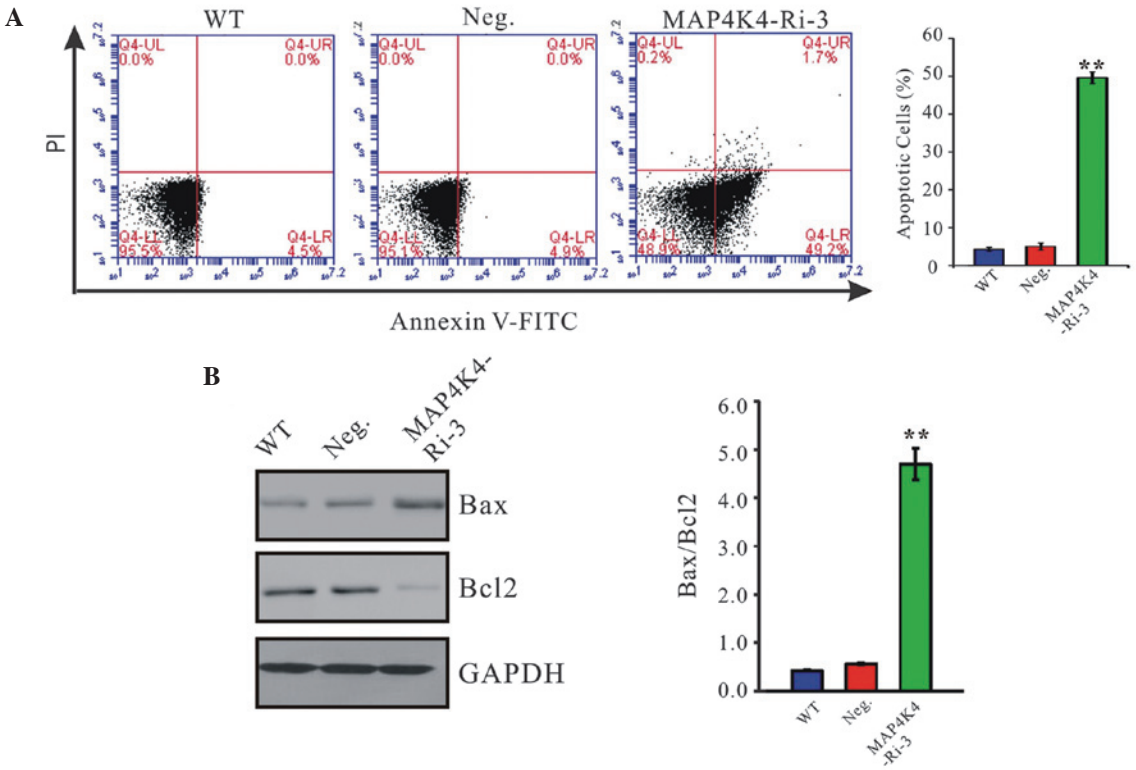

Figure 4. MAP4K4 knockdown induces cell apoptosis by increasing the Bax/Bcl-2 ratio. (A) Results of the annexin V-FITC/PI staining performed in control cells and MAP4K4 knockdown cells. MAP4K4 knockdown markedly induced cell apoptosis. (B) The Bax/Bcl-2 protein ratio was significantly increased in MAP4K4 RNAi cells. The data were expressed as the mean ± standard deviation (**P<0.01). WT, wild type cells; Neg., negative control; MAP4K4-Ri-3, MAP4K4-shRNA-3 virus-infected cells; FITC, fluorescein isothiocyanate; PI, propidium iodide; sh, short hairpin.

under a microscope (CX41RF; Olympus Corporation, Tokyo, Japan). The number of migrated cells was expressed as the mean ± standard deviation.

Statistical analysis. The data are expressed as the mean ± standard deviation. Statistical analyses were performed using GraphPad Prism 5 software (GraphPad Software, Inc., La

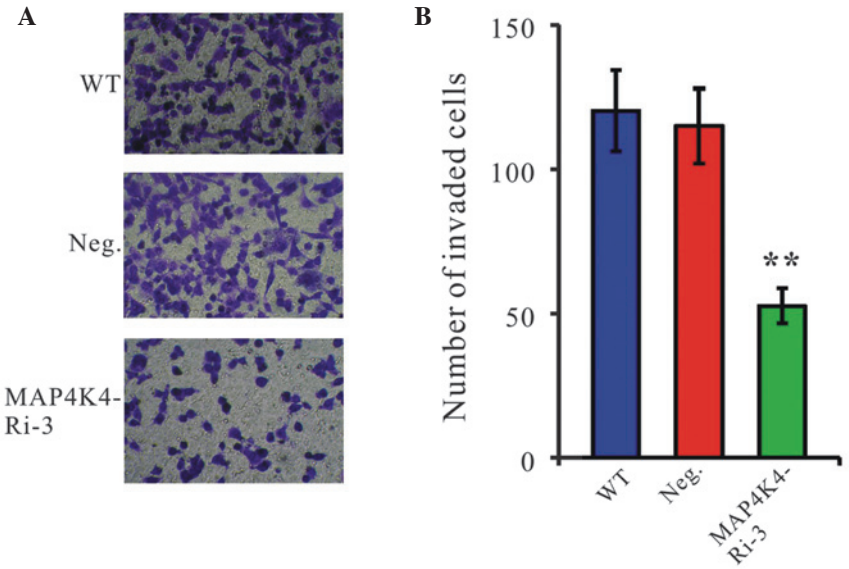

Figure 5. Suppressing the expression of MAP4K4 inhibits the invasiveness of hepatocellular carcinoma cells. An invasion assay of control and MAP4K4 knock-down BGC-823 cells in Matrigel-coated transwell chambers was performed. The cells, which migrated from the upper well of a Transwell chamber into the lower well were (A) stained and images were captured, and (B) subsequently quantified. The data are expressed as the mean ± standard deviation (**P<0.01). WT, wild-type; Neg., negative control; MAP4K4-Ri-3, MAP4K4-shRNA-3 virus-infected cells.

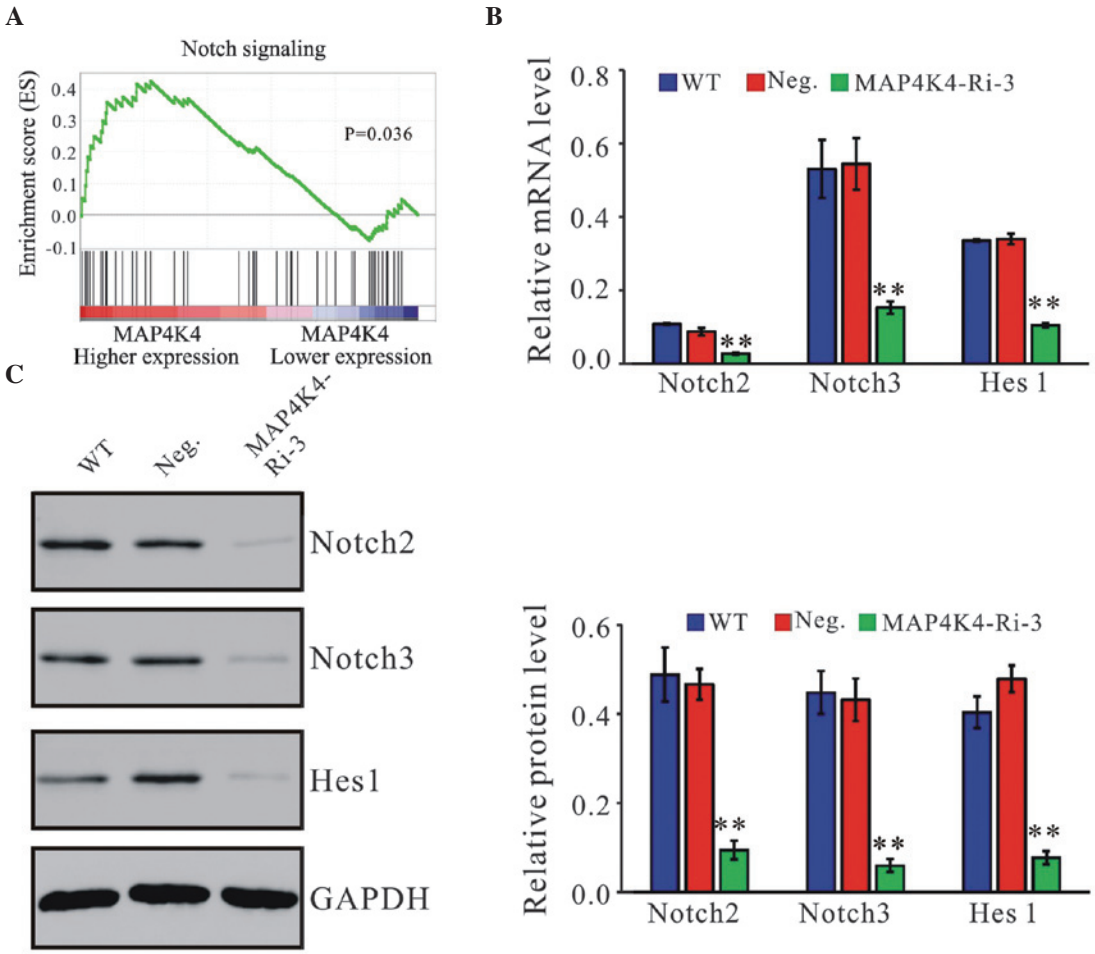

Figure 6. GSEA enrichment plot of KEGG Notch signaling pathway genes and MAP4K4 RNAi decreased gene expression. (A) Genes in the KEGG Notch signaling pathway revealed a significant enrichment in patients with a higher expression of MAP4K4 compared with patients with lower expression. The top portion of the figure plots the enrichment scores for each gene and the bottom portion of the plot shows the value of the ranking, moving down the list of ranked genes. (B) Reverse transcription-quantitative polymerase chain reaction and (C) western blot analysis revealed that the expression levels of Notch2, Notch3 and Hes1 were significantly reduced by MAP4K4 RNAi. The data are expressed as the mean ± standard deviation (**P<0.01). KEGG, Kyoto Encyclopedia of Genes and Genomes; RNAi, RNA interference; WT, wild-type; Neg., negative control; MAP4K4-Ri-3, MAP4K4-shRNA-3 virus-infected cells.

Jolla, CA, USA). The paired, two-tailed Student's t-test was used to analyze the significance of the difference between groups. $P<0.05$ was considered to indicate a statistically significant difference.

Results

MAP4K4 mRNA is overexpressed in GC. To determine whether MAP4K4 was overexpressed in GC, the mRNA expression of MAP4K4 in GC and adjacent tissues was analyzed by bioinformatics. As shown in Fig. 1A, the mRNA expression levels of MAP4K4 were significantly increased in GC tissues compared with the adjacent tissues of patients from TCGA stomach adenocarcinoma data-sets, which indicated that MAP4K4 may be an oncogene in GC.

To further determine the expression of MAP4K4 in GC, RT-qPCR analysis was performed on 25 pairs of GC and their matched non-cancerous tissue samples. Overexpressed levels of MAP4K4 mRNA were identified in 72% (18/25) of the assessed GC tissues (Fig. 1B). Statistical analysis revealed that the MAP4K4 mRNA was significantly overexpressed in gastric tumor tissues as compared with the normal tissues ($P<0.001$).

MAP4K4 is downregulated by RNAi in GC cells. The protein expression of MAP4K4 was also detected in five GC cell lines by western blotting. A high expression level of MAP4K4 was observed in the BGC-823 cells (Fig. 2A); consequently, BGC-823 cells were selected for the further analysis.

To investigate the function of MAP4K4 on GC, shRNA plasmids were constructed for the downregulation of MAP4K4 expression. A total of three pairs of human MAP4K4 gene shRNA sequences and a non-specific scrambled shRNA sequence, negative control (Neg.), were cloned into a lentiviral plasmid. The recombinant lentivirus was packaged into HEK-293T cells. BGC-823 cells were subsequently infected with MAP4K4-RNAi or Neg. virus. The silencing effect of the MAP4K4-RNAi was confirmed by western blotting (Fig. 2B) and RT-qPCR (Fig. 2C). MAP4K4-Ri-3 was identified as the most efficient infected cell type, and was used for subsequent experiments.

Downregulation of MAP4K4 by RNAi inhibits cell proliferation and induces G1 phase cell cycle arrest in GC cells. To determine the role of MAP4K4 downregulation in the proliferation of hepatocellular carcinoma cells, the proliferation of BGC-823 cells infected with MAP4K4-Ri-3 was analyzed using a CCK-8 assay. As shown in Fig. 3A, cell growth was markedly impaired in the MAP4K4-Ri-3 virus-infected cells (MAP4K4-Ri-3) compared with the wild-type cells (WT) and scrambled shRNA virus-infected cells (Neg.). These data indicated a role for MAP4K4 in the proliferation of GC cells.

Subsequently, the potential inhibitory effect of MAP4K4 knockdown on cell cycle progression was investigated. As shown in Fig. 3B, the suppression of MAP4K4 overexpression resulted in a higher number of cells in the G1 phase (64.9±2.9%) compared with the WT (46.0±2.8%) and Neg. cells (44.9±1.7%). There was a concomitant reduction in the number of cells in the S and G2-M phases. These data suggested that the knockdown of MAP4K4 induced cell cycle arrest in G1 in GC cells, which may be associated with the inhibition of cell proliferation in MAP4K4-Ri-3 cells.

MAP4K4 knockdown induces cell apoptosis by increasing the ratio of Bax/Bcl-2. To assess the effects of MAP4K4 on cell apoptosis, annexin V/PI staining was performed (Fig. 4A). The ratio of cells undergoing apoptosis was significantly increased to 49.6±1.5% in MAP4K4-Ri-3 cells compared with the WT (4.3±0.5%) and Neg. cells (5.0±1.0%). These data suggested that MAP4K4 may fulfil an antiapoptotic role in GC cells.

The proteins of the Bcl-2 family perform critical roles in the regulation of apoptosis by functioning as promoters (e.g. Bax) or as inhibitors (e.g. Bcl-2) of cell death processes (12-14). Western blotting was performed to detect the protein expression levels of Bcl-2 and Bax in the MAP4K4-Ri-3 cells (Fig. 4B). MAP4K4 knockdown resulted in a marked reduction in the level of the antiapoptotic protein, Bcl-2, with a concomitant increase in the level of proapoptotic protein Bax, compared with the control cells (WT and Neg.). These data revealed that the suppression of MAP4K4 expression may increase the ratio of Bax/Bcl-2, which may contribute to the increase in cell apoptosis.

Downregulation of MAP4K4 by RNAi inhibits the invasiveness of GC cells. To examine whether MAP4K4 affected the invasive ability of GC cells, a Matrigel-coated membrane chamber invasion assay was performed. As shown in Fig. 5, a markedly reduced invasive ability was observed in MAP4K4 knockdown cells compared with the control cells. The number of invading MAP4K4-Ri-3 cells was 44% compared with the Neg. cells (WT, 120±14; Neg., 115±13; MAP4K4-Ri-3, 53±6).

MAP4K4 positively correlates with the Notch signaling pathway. To further investigate the biological pathways involved in the pathogenesis of GC stratified by the median of MAP4K4 expression level, a GSEA analysis was performed. The enrichment plots of GSEA revealed that the MAP4K4 signature was positively correlated with the Notch signaling pathway (Fig. 6A). The gene expression patterns of important regulators in the Notch signaling pathway were determined at the mRNA and protein expression levels. The mRNA (Fig. 6B) and protein levels (Fig. 6C) of Notch2, Notch3 and Hes1 were markedly decreased following the downregulation of MAP4K4.

Discussion

MAPKs have an essential role in modulating the regulation of several important cellular processes, including growth, migration, differentiation, apoptosis and stress-associated responses. The involvement of MAP4K4 in cancer has generated great interest. High expression levels of MAP4K4 have been reported in several cancer types (5,8-10). The molecular mechanisms underlying the development and progression of GC remain to be fully elucidated. Consistent with these previous studies, the bioinformatics analysis in the present study, using data from TCGA, indicated that MAP4K4 was highly expressed in GC (Fig. 1A), which was further confirmed by RT-qPCR (Fig. 1B).

In the present study, MAP4K4 was subsequently knocked down in BGC-823 cells using RNAi (Fig. 2). The data revealed that suppressing MAP4K4 expression markedly inhibited the proliferation (Fig. 3) and the invasion (Fig. 5) of BGC-823 cells, which is consistent with previous reports in pancreatic cancer (15) and hepatocellular carcinoma (9). These data further indicated the importance of MAP4K4 in gastric cell carcinogenesis.

Cell cycle regulation is frequently abnormal in the majority of the common malignancies, resulting in aberrant cell proliferation (16,17). Silencing of MAP4K4 by RNAi markedly induced G1 phase arrest of cell cycle progression (Fig. 3B), which indicated that the inhibition of cell proliferation in GC cells is due to the inhibition of cell cycle progression.

The G1 phase arrest of cell cycle progression provides an opportunity for the cells to either undergo repair, or to enter into apoptosis. The effects of knockdown of the MAP4K4 protein on the induction of apoptosis were subsequently determined in BGC-823 cells. The flow cytometry data revealed that the silencing of MAP4K4 resulted in a marked induction of apoptosis (Fig. 4A). Apoptosis is of major importance during the elimination of the mutated neoplastic and hyperproliferating neoplastic cells, and therefore, is considered as a protective mechanism against cancer progression (18). Due to its anti-apoptotic role in GC, MAP4K4 may be a putative therapeutic target worthy of further investigation.

The proteins of the Bcl-2 family either promote cell survival (e.g. Bcl-2) or induce programmed cell death (e.g. Bax). The ratio of Bax/Bcl-2 is critical for the induction of apoptosis, and this ratio determines whether cells undergo apoptosis (14). The present study revealed that MAP4K4 knockdown resulted in an increase in the expression of Bax and a decrease in the expression of Bcl-2 (Fig. 4B), and the ratio of Bax/Bcl-2 was increased (Fig. 4B), which suggested that MAP4K4 exerted its antiapoptotic role by regulating the ratio of Bax/Bcl-2.

The GSEA indicated that the overexpression of MAP4K4 correlates with the activation of the Notch signaling pathway (Fig. 6A). The Notch pathway is an evolutionarily conserved cell signaling mechanism, which is involved in several cellular processes, including proliferation, differentiation, apoptosis and stem cell maintenance (19). Dysregulation of Notch signaling was reported in several cancer types (20-22). It was reported that Notch2 (23,24) and Notch3 (25) are important in controlling the progression of GC. Hes1, a target gene of Notch signaling activation, is considered to be critical for the development of prostate cancer (26-28). In the present study, MAP4K4 knockdown markedly decreased the mRNA (Fig. 6B) and protein expression levels (Fig. 6C) of Notch2, Notch3 and Hes1, which indicated an association between MAP4K4 function and the regulation of Notch signaling in GC cells.

In conclusion, the results of the present study indicated that MAP4K4 knockdown inhibited cell proliferation via induction of the G1 phase arrest. Mechanistic evidence has been provided to demonstrate that cell apoptosis induced by MAP4K4 RNAi was mediated through an increase in the ratio of Bax/Bcl2. Additionally, MAP4K4 was positively correlated with the Notch signaling pathway in GC, and therefore may provide useful information for the development of targeted therapeutic strategies in the future.

References

1. Vogelaar IP, van der Post RS, Bisseling TM, van Krieken JH, Ligtenberg MJ and Hoogerbrugge N: Familial gastric cancer: Detection of a hereditary cause helps to understand its etiology. Hered Cancer Clin Pract 10: 18, 2012.
2. Jemal A, Clegg LX, Ward E, Ries LA, Wu X, Jamison PM, Wingo PA, Howe HL, Anderson RN and Edwards BK: Annual report to the nation on the status of cancer, 1975-2001, with a special feature regarding survival. Cancer 101: 3-27, 2004.
3. Turjanski AG, Vaqué JP and Gutkind JS: MAP kinases and the control of nuclear events. Oncogene 26: 3240-3253, 2007.
4. Collins CS, Hong J, Sapinoso L, Zhou Y, Liu Z, Micklash K, Schultz PG and Hampton GM: A small interfering RNA screen for modulators of tumor cell motility identifies MAP4K4 as a promigratory kinase. Proc Natl Acad Sci USA 103: 3775-3780, 2006.
5. Wright JH, Wang X, Manning G, LaMere BJ, Le P, Zhu S, Khatry D, Flanagan PM, Buckley SD, Whyte DB, *et al*: The STE20 kinase HGK is broadly expressed in human tumor cells and can modulate cellular transformation, invasion and adhesion. Mol Cell Biol 23: 2068-2082, 2003.
6. Hu Y, Leo C, Yu S, Huang BC, Wang H, Shen M, Luo Y, Daniel-Issakani S, Payan DG and Xu X: Identification and functional characterization of a novel human misshapen/Nck interacting kinase-related kinase, hMINK beta. J Biol Chem 279: 54387-54397, 2004.
7. Zohn IE, Li Y, Skolnik EY, Anderson KV, Han J and Niswander L: p38 and a p38-interacting protein are critical for downregulation of E-cadherin during mouse gastrulation. Cell 125: 957-969, 2006.
8. Liang JJ, Wang H, Rashid A, Tan TH, Hwang RF, Hamilton SR, Abbruzzese JL, Evans DB and Wang H: Expression of MAP4K4 is associated with worse prognosis in patients with stage II pancreatic ductal adenocarcinoma. Clin Cancer Res 14: 7043-7049, 2008.
9. Liu AW, Cai J, Zhao XL, Jiang TH, He TF, Fu HQ, Zhu MH and Zhang SH: ShRNA-targeted MAP4K4 inhibits hepatocellular carcinoma growth. Clin Cancer Res 17: 710-720, 2011.
10. Qiu MH, Qian YM, Zhao XL, Wang SM, Feng XJ, Chen XF and Zhang SH: Expression and prognostic significance of MAP4K4 in lung adenocarcinoma. Pathol Res Pract 208: 541-548, 2012.
11. Sun M, Xia R, Jin F, Xu T, Liu Z, De W and Liu X: Downregulated long noncoding RNA MEG3 is associated with poor prognosis and promotes cell proliferation in gastric cancer. Tumour Biol 35: 1065-1073, 2014.
12. Adams JM and Cory S: Life-or-death decisions by the Bcl-2 protein family. Trends Biochem Sci 26: 61-66, 2001.
13. Hetz C: BCL-2 protein family. Essential regulators of cell death. Preface. Adv Exp Med Biol 687: vii-viii, 2010.
14. Reed JC: Regulation of apoptosis by bcl-2 family proteins and its role in cancer and chemoresistance. Curr Opin Oncol 7: 541-546, 1995.
15. Zhao G, Wang B, Liu Y, Zhang JG, Deng SC, Qin Q, Tian K, Li X, Zhu S, Niu Y, *et al*: miRNA-141, downregulated in pancreatic cancer, inhibits cell proliferation and invasion by directly targeting MAP4K4. Mol Cancer Ther 12: 2569-2580, 2013.
16. Evan GI and Vousden KH: Proliferation, cell cycle and apoptosis in cancer. Nature 411: 342-348, 2001.
17. Molinari M: Cell cycle checkpoints and their inactivation in human cancer. Cell Prolif 33: 261-274, 2000.
18. Hanahan D and Weinberg RA: Hallmarks of cancer: The next generation. Cell 144: 646-674, 2011.
19. Koch U and Radtke F: Notch and cancer: A double-edged sword. Cell Mol Life Sci 64: 2746-2762, 2007.
20. Nickoloff BJ, Osborne BA and Miele L: Notch signaling as a therapeutic target in cancer: A new approach to the development of cell fate modifying agents. Oncogene 22: 6598-6608, 2003.
21. Westhoff B, Colaluca IN, D'Ario G, Donzelli M, Tosoni D, Volorio S, Pelosi G, Spaggiari L, Mazzarol G, Viale G, *et al*: Alterations of the Notch pathway in lung cancer. Proc Natl Acad Sci USA 106: 22293-22298, 2009.
22. Stylianou S, Clarke RB and Brennan K: Aberrant activation of notch signaling in human breast cancer. Cancer Res 66: 1517-1525, 2006.
23. Tseng YC, Tsai YH, Tseng MJ, Hsu KW, Yang MC, Huang KH, Li AF, Chi CW, Hsieh RH, Ku HH and Yeh TS: Notch2-induced COX-2 expression enhancing gastric cancer progression. Mol Carcinog 51: 939-951, 2012.

24. Bauer L, Langer R, Becker K, Hapfelmeier A, Ott K, Novotny A, Höfler H and Keller G : Expression profiling of stem cell-related genes in neoadjuvant-treated gastric cancer: A NOTCH2, GSK3B and β-catenin gene signature predicts survival. PLoS One 7: e44566, 2012.
25. Kang H, An HJ, Song JY, Kim TH, Heo JH, Ahn DH and Kim G: Notch3 and Jagged2 contribute to gastric cancer development and to glandular differentiation associated with MUC2 and MUC5AC expression. Histopathology 61: 576-586, 2012.
26. Lu JP, Zhang J, Kim K, Case TC, Matusik RJ, Chen YH, Wolfe M, Nopparat J and Lu Q: Human homolog of Drosophila Hairy and enhancer of split 1, Hes1, negatively regulates δ-catenin (CTNND2) expression in cooperation with E2F1 in prostate cancer. Mol Cancer 9: 304, 2010.
27. Leong KG and Gao WQ: The Notch pathway in prostate development and cancer. Differentiation 76: 699-716, 2008.
28. Villaronga MA, Bevan CL and Belandia B: Notch signaling: A potential therapeutic target in prostate cancer. Curr Cancer Drug Targets 8: 566-580, 2008.